Separation Science and Technology
Publication details, including instructions for authors and subscription information:
http://www.informaworld.com/smpp/title~content=t713708471

CONCENTRATION OF NaCl SOLUTION BY MEMBRANE DISTILLATION INTEGRATED WITH CRYSTALLIZATION

Marek Gryta[a]
[a] Technical University of Szczecin, Institute of Chemical and Environment Engineering, Szczecin, Poland

Online publication date: 23 October 2002

To cite this Article Gryta, Marek(2002) 'CONCENTRATION OF NaCl SOLUTION BY MEMBRANE DISTILLATION INTEGRATED WITH CRYSTALLIZATION', Separation Science and Technology, 37: 15, 3535 — 3558
To link to this Article: DOI: 10.1081/SS-120014442
URL: http://dx.doi.org/10.1081/SS-120014442

MARCEL DEKKER, INC. • 270 MADISON AVENUE • NEW YORK, NY 10016

SEPARATION SCIENCE AND TECHNOLOGY
Vol. 37, No. 15, pp. 3535–3558, 2002

CONCENTRATION OF NaCl SOLUTION BY MEMBRANE DISTILLATION INTEGRATED WITH CRYSTALLIZATION

Marek Gryta*

Technical University of Szczecin, Institute of Chemical and Environment Engineering, ul. Pułaskiego 10, 70-322 Szczecin, Poland

ABSTRACT

Concentration of NaCl solutions by direct-contact membrane distillation (DCMD) integrated with salt crystallization has been studied. The salt crystallization was carried out in a batch mode or continuously. The influence of process parameters (flow rates, temperatures, and concentrations) on permeate flux has been investigated. To evaluate the polarization phenomena, a simple model was used. This model showed good agreement with the experimental results. Two types of membrane distillation MD capillary modules, with the membranes arranged in a form of braided capillaries or helically wounded, were tested. The membrane wettability during long-term testing was investigated. A slow decline of the module efficiency was observed since the membranes were partially wetted during the process. The MD

*E-mail: margryta@mailbox.tuniv.szczecin.pl

DOI: 10.1081/SS-120014442
0149-6395 (Print); 1520-5754 (Online)

www.dekker.com

MARCEL DEKKER, INC. • 270 MADISON AVENUE • NEW YORK, NY 10016

process integrated with continuous crystallization yielded an average NaCl production of $100\,kg\,m^{-2}\,d^{-1}$.

Key Words: Membrane distillation; Salt crystallization; Capillary module; Hydrophobic membrane; NaCl

INTRODUCTION

One of the noxious wastes produced by the industry comprises the dilute solutions of salts, particularly NaCl. These solutions are difficult for the treatment, therefore, they are frequently discharged into the environment. This is a reason for environmental damage and an increase in the surface water salinity.[1] The major sources of saline wastewater production comprise coalmines and power plants. The salt concentration in discharged wastewater is not generally high, within the range $5–50\,g\,dm^{-3}$, thus a problem results from their toxicity and huge amounts of wastes. It was estimated that more than 4.8×10^9 kg of salts (mainly NaCl) is annually discharged into the Vistula and Odra rivers (Poland) solely from the mines.[2] Taking into consideration the impact of such wastewater on the environment, the treatment restricted only to the concentration is insufficient. Therefore, the obtained concentrate should be treated before the disposal. One of the solutions may comprise the separation of salt in the solid state, followed by its utilization as a raw material or safely disposed.

The separation of salt from aqueous solutions is carried out most frequently using the thermal methods, such as multi-stage flash evaporation (MSF), multi-effect distillation (MED), and vapor compression (VC).[1–3] Considering the energy consumption, these processes are essentially used for the concentration of brines. Reverse osmosis (RO) can be employed for a preliminary concentration of saline wastewater, thus the cost of the thermal methods will be considerably reduced and the range of their application can include the diluted solutions.[1–4] However, the RO process requires the application of a sophisticated pretreatment due to the considerable problems associated with the fouling and scaling. The applications of nanofiltration (NF) or a combine ultrafiltration/nanofiltration (UF/NF) system, to separate the divalent ions, allows limiting the scaling phenomenon (mainly $CaSO_4$) and the concentration factor in the RO process can be enhanced.[2,4] The possibility of application of integrated membrane systems to solve the problem of saline wastewater treatment is the subject of ongoing studies.

One of the new methods used to concentrate the salt solutions is membrane distillation (MD) process.[5–7] In this process, a hydrophobic membrane

separates a hot solution (feed) from a cold distillate, direct-contact membrane distillation (DCMD). The volatile components evaporated from the feed are transported across the pores of nonwetted membrane, and subsequently they are condensed on the other side of the membrane. The experimental results demonstrate a good perspective of MD application for the treatment of spent metal pickling solutions,[8] and for a continuous production of ethanol in MD membrane bioreactor.[9] The major advantage of the MD process is its capability to concentrate the salt up to the supersaturated state, which allows the crystallization of salt.[8,10,11]

The maintenance of the gas phase in the membrane pores is a principal condition required to carry out the MD process. The utilization of the membranes manufactured from polymers such as polytetrafluoroethylene, poly(vinylidene fluoride) or polypropylene, with the pore diameter within the range 0.1–1.0 μm, permits to comply with the condition of being nonwetted in the MD process by various aqueous solutions. However, a preparation of supersaturated solutions by MD process can facilitate the wettability of the membrane.[7] The selection of appropriate parameters to run the MD integrated with the crystallization process in order to prevent the membrane wetting was the major objective of this work.

THEORY

Heat and Mass Transfer

The separation mechanism in the MD process is based on the vapor/liquid equilibrium of solution. In the case of a solution containing nonvolatile solutes, e.g., NaCl, only water vapor flows through the membrane. Therefore, the MD process can be used for the treatment of saline wastewater to convert it to pure water and to the concentrate containing the components present in the mother liqueur. The driving force for the mass transfer is the vapor pressure difference across the membrane ($\Delta p = p_F - p_D$), caused by both the existing temperature gradient ($\Delta T = T_1 - T_2$) and the composition of solutions (c_1, c_D) in the layers adjacent to the membrane (Fig. 1).

The mass stream flowing through the membrane can be described by the equation obtained from the general (Maxwell's) diffusion equation:[12,13]

$$J = \frac{\varepsilon M D_E P}{\chi s R T_m} \ln \frac{P - p_D}{P - p_F} \tag{1}$$

where ε, χ, s, T_m are the porosity, tortuosity, thickness, and the mean temperature of the membrane, respectively, M, the molecular weight of water, R, the gas

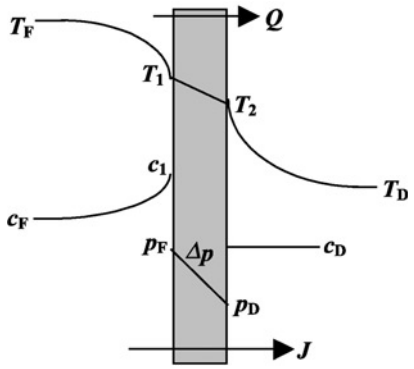

Figure 1. Model of DCMD process.

constant, P, the total pressure, D_E, the effective diffusion coefficient of water vapor through the membrane pores, and J is the water flux.

The temperatures of surface adjacent to the membrane can be calculated from the following expression:[14]

$$T_1 = \frac{\alpha_F T_F(1 - e^{-Jc_p s/\lambda_m}) + Jc_p\left(\frac{\alpha_F}{\alpha_D}T_F + T_D\right) - JH(1 - e^{-Jc_p s/\lambda_m})}{\alpha_F(1 - e^{-Jc_p s/\lambda_m}) + Jc_p\left(1 + \frac{\alpha_F}{\alpha_D}\right)} \quad (2)$$

$$T_2 = \frac{\alpha_D T_D(1 - e^{-Jc_p s/\lambda_m}) + Jc_p\left(\frac{\alpha_D}{\alpha_F}T_D + T_F\right) + JH(1 - e^{-Jc_p s/\lambda_m})}{\alpha_D(1 - e^{-Jc_p s/\lambda_m}) + Jc_p\left(1 + \frac{\alpha_D}{\alpha_F}\right)} \quad (3)$$

where $H = f(T_2)$ is the vapor enthalpy, α_i, the convective heat transfer coefficients, c_p, the vapor specific heat, and λ_m is the membrane thermal conductivity. The α_i coefficients can be estimated from the Nusselt number: $Nu = \alpha d_h/\lambda$, where d_h is the hydraulic diameter and λ is the solution thermal conductivity.

The effect of salt concentration on the partial vapor pressure can be taken into account by:

$$p = p^0(1 - x)\gamma \quad (4)$$

where x is the mole fraction of salt and γ is the activity coefficient, for NaCl solution given by:[15]

$$\gamma = 1 - 0.5x - 10x^2 \quad (5)$$

The evaporation of water causes an increase in salt concentration at the feed/membrane interface (concentration polarization phenomenon). According to the film theory, the salt concentration in the bulk phase (c_F), and at the feed/membrane interface (c_1) are related to the flux by:[16]

$$c_1 = c_F \exp\left(\frac{J_V}{k_M}\right) \tag{6}$$

where k_M is the mass transfer coefficient of salt in the feed. This equation is valid when the total salt rejection is observed. It was generally obtained for separation of NaCl solutions by MD,[5,11] and in this case that the assumption on the distillate side flow distilled water is correct. The coefficient k_M can be obtained from the Chilton–Colburn analogy, which relates the mass transfer to the heat transfer as:[17]

$$Sh\, Sc^{-0.33} = Nu\, Pr^{-0.33} \tag{7}$$

where the Sherwood number is $Sh = k_M d_h / D_S$, the Schmidt number is $Sc = \mu/\rho D_S$, the Prandtl number is $Pr = c_{PS}\mu/\lambda$, where D_S is the salt diffusion coefficient and μ, ρ, c_{PS} are the viscosity, the density, and the specific heat of solution, respectively.

Nusselt number correlations development for the heat exchangers were successfully used for heat transfer calculation in MD modules.[14] This number can be given by the empirical correlation due to Sider and Tate for the dimensionless numbers:[18]

$$Nu = 1.86\left(Re\, Pr \frac{d_h}{L}\right)^{0.33}\left(\frac{\mu}{\mu_W}\right)^{0.14} \tag{8}$$

where the Reynolds number is $Re = v d_h \rho/\mu$, L is the module length and v is the flow rate. Equation (8) is often used for the estimation of heat transfer coefficient in MD module.[12,13,19] The calculations are based on the arithmetic mean of the inlet and outlet temperature differences. Moreover, all the fluid properties are evaluated at the mean bulk temperature of streams, except μ_W, which is evaluated at the wall (membrane) temperature. This relationship is valid for the short tubes and forced convection, i.e., for the membrane modules shorter than the thermal and velocity entry lengths in laminar flow, $Re\, Pr\, d_h/L > 10$.[18] If this term is smaller than 10, then the Nu number can be estimated from the correlation:[20]

$$Nu = 0.5\left(Re\, Pr \frac{d_h}{L}\right)\left(\frac{\mu}{\mu_W}\right)^{0.14} \tag{9}$$

For the transition region ($2000 < Re < 10{,}000$) the following correlation was proposed by Hausen:[20]

$$Nu = 0.116(Re^{0.66} - 125)Pr^{0.33}\left(1 + \left(\frac{d_h}{L}\right)^{0.66}\right)\left(\frac{\mu}{\mu_W}\right)^{0.14} \quad (10)$$

The capillary modules with the membranes arranged in a form of braided capillaries or helically wounded were found more efficient than that with parallel arrangement.[21–24] The heat and mass transfer coefficients obtained in these designs with the laminar flow were of the same order of magnitudes as turbulent flow in straight ducts. Therefore, the correlations used for the estimation of *Nu* or *Sh* numbers have the exponents in the range 0.4–1.0.[24] For module with helically wound capillaries the following relationship can be used:

$$Nu = 0.15Re^{0.8}Pr^{0.33} \quad (11)$$

Membrane Wetting

During the operation of the MD process, a fraction of the membrane pores becomes filled by the feed as a result of the feed/membrane interaction. The presence of salts in the feed significantly affects the membrane wettability.[11,25] In the MD process, the salt solution flows through a module and is simultaneously concentrated and cooled. This may lead to the formation of the salt crystals on the membrane surface[5,6,11] resulting in the wetting of the membrane fragments occupied by the crystals. The phenomena of temperature and concentration polarizations significantly facilitate the salt nucleation on the membrane surface. The supersaturation state of solution was also reached inside the pores (partially filled by the feed) due to the evaporation of water, as well as a result of impeded diffusion of solutes from the liquid/vapor interface into the bulk of feed.[26] The salt crystallization is possible under these conditions, thereby the entire pore volume can be filled by the feed (Fig. 2). As a consequence, the convective and/or diffusive transport of solutes through the wetting pores from the feed to distillate is possible, and can lead to the contamination of distillate. Therefore, during the MD process one should select such a feed concentration and the stream temperatures, which prevent the supersaturation of salt in the layer adjacent to the membrane on the feed side. An essential inconvenience encountered during the concentration of NaCl solutions is associated with the solubility of this salt, which is slightly dependent on the temperature (Fig. 3).[27,28] Thereby, the prevention of salt crystallization inside MD module by the temperature program becomes more difficult. The module design also plays a significant role. The configuration comprising the capillary membranes packed in a spiral mode[21] or braided mode[22] ensures the achievement of appropriate hydrodynamic

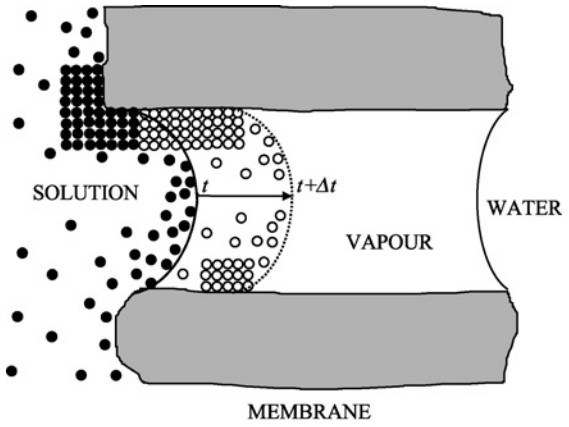

Figure 2. Model of membrane wetting induced by the formation of salt deposit inside the pores during the concentration of salt solution. Solute: ●, initial; ○, after Δt.

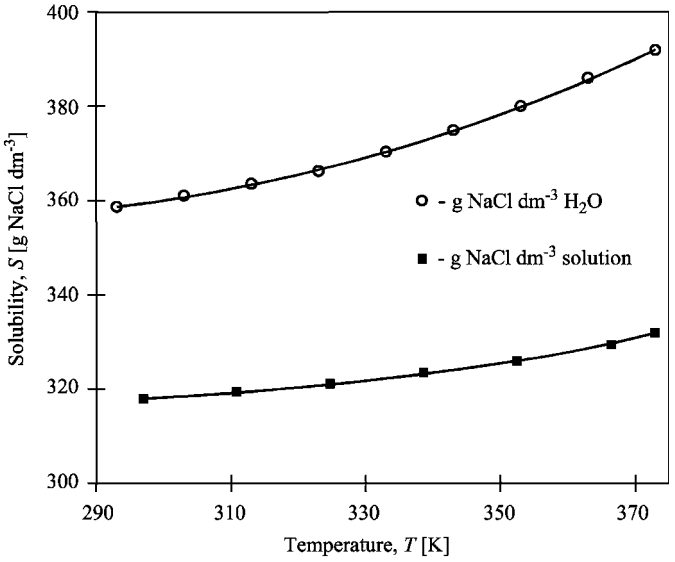

Figure 3. The effect of solution temperature on NaCl solubility. The curves plotted on the basis of Ref. [27], ○ and Ref. [28], ■.

conditions in the module. Therefore, the temperature and concentration polarization phenomena are restricted, and the salt crystallization inside the module could be limited.

EXPERIMENTAL

The MD studies concerning the concentration of NaCl solutions were carried out with periodical (Mode I) and continuous (Mode II) crystallization of salt. In the first mode, a part of diluted salt solution (2.5 dm^3) was concentrated up to the state close to the saturation. Subsequently, a fresh part of diluted solution replaced the obtained brine. The MD installation was operated in this mode for 6–8 hr/day. The brine removed from MD installation was cooled to 295K, and then subjected to the crystallization of salt. The crystallized salt was separated by filtration after 20 hr, and was weighted. The supernatant liquid (1.5 dm^3) was supplemented with a part (1 dm^3) of mother liqueur (20–100 g NaCl dm^{-3}), and this mixture constituted a fresh portion of diluted solution subjected to a further concentration according to Mode I.

The studies with continuous crystallization of salt (Mode II) were performed using the same installation as in Mode I. However, in this case the feed tank was replaced by a crystallizer composed of the three tanks connected in line, each having 3 dm^3 of volume (Fig. 4). The temperatures in these tanks were 323, 290, and 353K, respectively. A feeding salt solution was supplied into the last

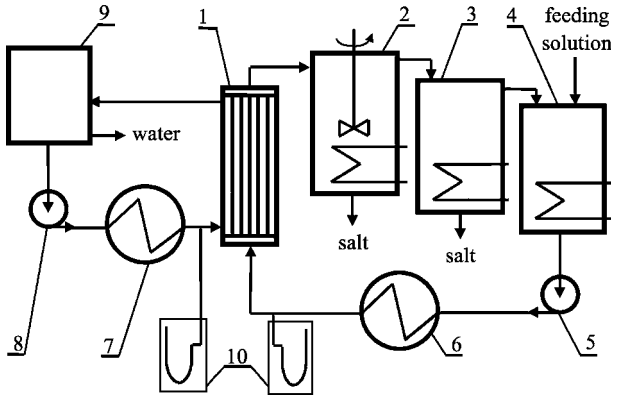

Figure 4. Diagram of the experimental set-up for DCMD integrated with crystallizer. 1, capillary module; 2, 3, 4, crystallization system; 5, 8, pump; 6, heating system; 7, cooling system; 9, distillate reservoir; 10, manometer.

tank in a continuous mode. The amount of salt separated in the crystallizer was calculated on the basis of distillate flux and the concentration of feeding solution (g NaCl $dm^{-3}H_2O$). The yield of crystallizer is associated with the membrane area of a given MD module, thus the amount of separated salt was calculated per unit of the membrane area and per elapsed time (kg NaCl $m^{-2} d^{-1}$). The volume of obtained distillate was determined every 2 hr, and the MD installation was operated for 6–10 hr/day. An experiment with a continuous operation (2 days) of the MD installation, both according to Mode I and Mode II, was also performed.

Three membrane modules (M1—Mode I and M2, M3—Mode II) with different dimensions were used. The capillary polypropylene membranes (Accurel S6/2 PP, Akzo Nobel) with outside/inside diameter equal to $d_{out}/d_{in} = 2.6/1.8$ mm were assembled in these modules. These membranes have pores size with the maximum and nominal diameter of 0.55 and 0.22 μm, respectively, and the porosity of 75% (manufacturer's data). The M1 and M2 modules were equipped with the nine membranes (0.52 and 0.55 m length, respectively) mounted in tubular housing with the inner diameter equal to 0.012 m. These membranes were assembled as a parallel bundle of braided capillaries (three membranes in braid). The M3 module with spiral wound capillary membranes was described in previous work.[21] In this module, 15 membranes with length of 0.565 m were spiral wound around the axial pipe (0.01 m outside diameter) and were then inserted into the tubular housing with the inner diameter equal to 0.022 m. These membrane modules were assembled in the MD installation in a vertical position. The feed and distillate streams flowed co-currently (5–14 $cm^3 sec^{-1}$) from the bottom to the upper part of MD module. The feed was circulated inside the capillary membranes. The feed temperature at the module inlet was varied in the range 333–358K, whereas the distillate temperature was varied in the range 293–328K. A technical grade NaCl was used for these studies. The feeding solutions containing 20–316 g NaCl dm^{-3} were prepared by dissolution of salt in distilled water. During the MD studies with a constant concentration of salt in the feed, the volume loss in the feed tank (equal to the permeate flux) were continuously supplemented by distilled water.

Variations of the maximal permeate flux during MD module operation were investigated periodically using distilled water as a feed. In this case, the distillate temperature amounted to 293K, whereas the feed temperature was 353K. The electrical conductivity and the total dissolved solids (TDS) of the examined solutions were measured by a 6P Ultrameter (Myron L Company). This instrument permits the direct measurement of the salt content (ppm) in solution containing up to 100 g NaCl dm^{-3}. Since the examined samples also contained a larger amount of salt, they were 10-fold diluted with distilled water before the analysis. A real concentration of salt was determined from the chart obtained on the basis of measurements with the reference solutions.

RESULTS AND DISCUSSION

Influence of Process Parameters

The efficiency of concentration process of NaCl solutions by MD is dependent on the temperature and concentration of streams flowing through the module, their flow rate, and the arrangement of capillary membranes in the module. All these parameters have a significant influence on the value of the driving force in the MD process.

The effect of salt concentration in the feed on permeate flux are shown in Fig. 5. The initial permeate flux, amounting to $575\,dm^3\,m^{-2}\,d^{-1}$ for distilled water, decreased to $342\,dm^3\,m^{-2}\,d^{-1}$ when the solute concentration in the feed increased to $305\,g\,NaCl\,dm^{-3}$. The observed decline of flux was caused by the reduction of the driving force for the mass transfer as a result of a decrease of the partial pressure of water vapor over the salt solution. The increase in solute concentration also affects the temperature and concentration polarization phenomena resulting in a decline of permeate flux.[16] The MD model presented in the theoretical part of this work describes the influence of all these parameters on the MD performance (Fig. 5). The axial changes of temperature and composition of the streams along the module for co-current flow were calculated from the balance equations, similarly as in the works of Gryta et al.[12–14] The

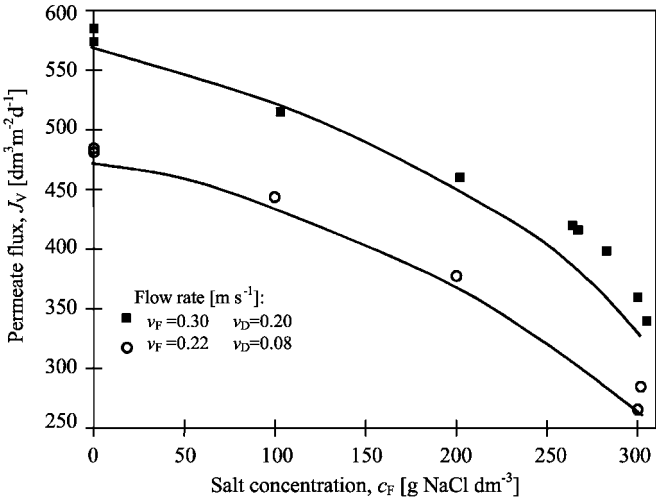

Figure 5. The effect of salt concentration in the feed on permeate flux (points). Lines—model predictions. The inlet temperature of streams: $T_{Fin} = 358K$, $T_{Din} = 293K$. Module M1.

heat transfer coefficients estimated from Eq. (9) were used for the calculation of interfacial temperatures T_1 and T_2. The physical properties of liquids (water and NaCl solutions), for various compositions and temperatures, required for the model calculations were found in the literature.[20,28] The shape of the modeling curves shown in Fig. 5 indicates that the presented model adequately describes the course of concentration process of NaCl solutions by MD.

The primary source of errors in the model analysis was the determination of the convective heat transfer coefficients. When the coefficients α_i were estimated from Eq. (8) a comparison of the experimental data and model predictions revealed that the errors are two times larger than that shown in Fig. 5, predicted for Eq. (9). The permeate flux, calculated on the basis of the model with Eqs. (8) or (9), was lower than its experimental value. These equations are adequate for the laminar flow in straight tubes, therefore, the enhancement of heat transfer in used module with braded capillaries cannot be correctly estimated. A higher value of α_i coefficients, due to the mixing effects, can be calculated by using Eq. (11). The model predictions for this equation were compared with the experimental data shown in Figs. 6–8. It can be concluded that a significantly better agreement was obtained in this case. However, in order to obtain the best agreement between the experimental and model results, one should use a special procedure for the selection of the Nusselt correlation for a given MD module.[14]

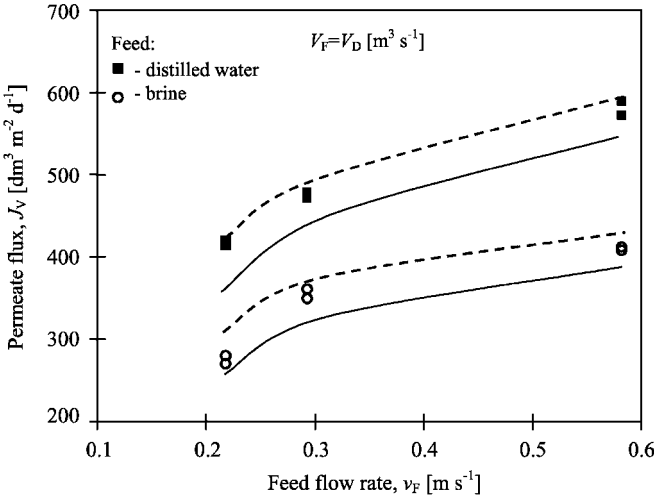

Figure 6. The effect of feed flow rate on permeate flux for the same volumetric flow rate of the feed and distillate. The inlet temperatures of streams: $T_{Fin} = 353$K and $T_{Din} = 293$K. The average brine concentration 250–260 g NaCl dm^{-3}. Model predictions: solid lines Eq. (9), dotted lines Eq. (11). Module M1.

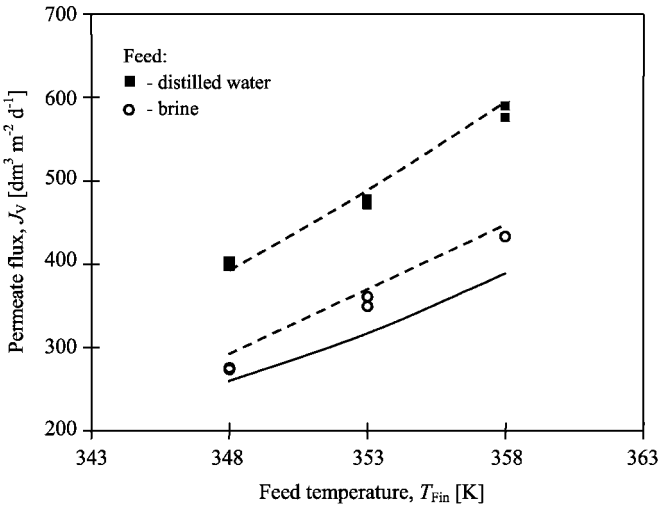

Figure 7. The effect of feed inlet temperature on permeate flux. The average brine concentration 250–260 g NaCl dm^{-3}. Distillate inlet temperature $T_{Din} = 293$K. Flow rates: $v_F = 0.3$ m sec^{-1} and $v_D = 0.1$ m sec^{-1}. Model predictions: solid lines Eq. (9), dotted lines Eq. (11). Module M1.

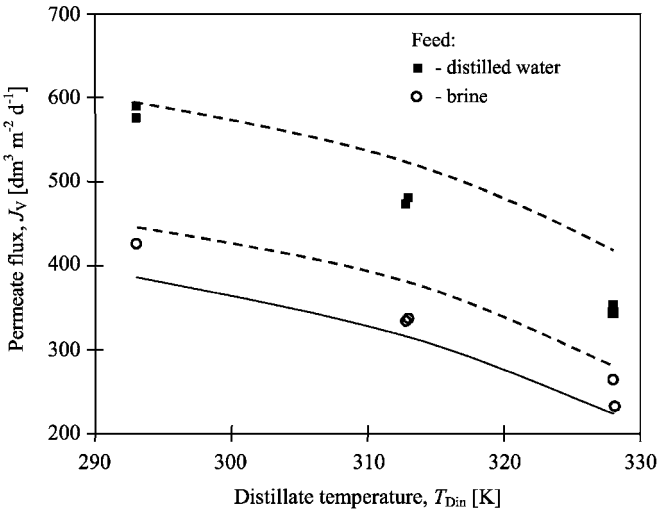

Figure 8. The effect of distillate inlet temperature on the permeate flux. The average brine concentration 250–260 g NaCl dm^{-3}. Feed inlet temperature $T_{Fin} = 358$K. Flow rates: $v_F = 0.3$ m sec^{-1} and $v_D = 0.1$ m sec^{-1}. Model predictions: solid lines Eq. (9), dotted lines Eq. (11). Module M1.

The results shown in Fig. 5 demonstrate that the flow rate of streams considerably affects the efficiency of salt concentration process. Generally, the efficiency of MD module increases with an increase of the flow rate. This effect is particularly significant for the feed velocity and is slightly smaller for the distillate velocity.[21] Moreover, an increase in the module efficiency caused by variation of the flow rate is limited. Therefore, for each type of MD module an optimum flow rate should be determined. The effect of the feed flow rate on the distillate flux for the module M1 is shown in Fig. 6. The enhancement v_F from $0.22\,m\,sec^{-1}$ ($v_D = 0.08\,m\,sec^{-1}$) to $0.58\,m\,sec^{-1}$ ($v_D = 0.2\,m\,sec^{-1}$) caused an increase of the efficiency from 255 to $410\,dm^3\,m^{-2}\,d^{-1}$ (for brine). The observed dependence of permeate flux on the flow rate is essentially due to two effects. Firstly, the values of the heat transfer coefficient α rise along with an increase of the flow rate, thus a negative influence of temperature polarization decreases. Secondly, an enhancement of the flow rate caused that the outlet temperatures of streams were closer to their temperatures at the module entrance, which also increases the driving force for mass transfer.[21] This driving force decreases with the module length, as a consequence of heat and mass transfer through the membranes. The changes of bulk temperatures and interfacial solution/membrane temperatures are shown in Fig. 9. An increase of the flow rate causes an increase of the temperature difference alongside the module. Thus, the value of the driving force for mass transfer increases with the increase of the flow rate (Fig. 10).

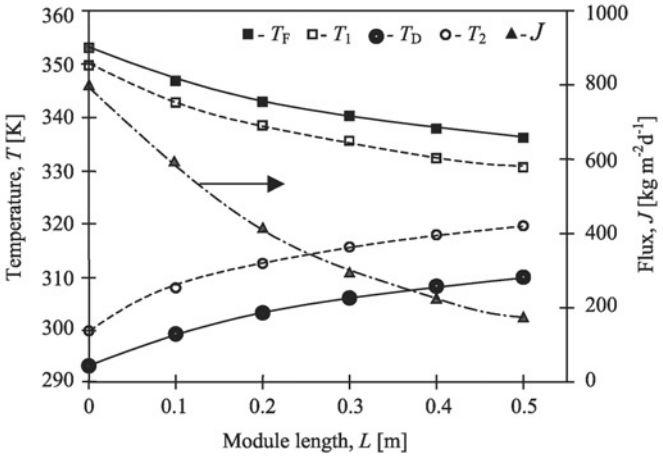

Figure 9. Variation of calculated temperatures of streams and permeate flux along the M1 module. Feed—distilled water. Flow rates: $v_F = 0.22\,m\,sec^{-1}$ and $v_D = 0.08\,m\,sec^{-1}$. $J_{Average} = 352\,kg\,m^{-2}\,d^{-1}$.

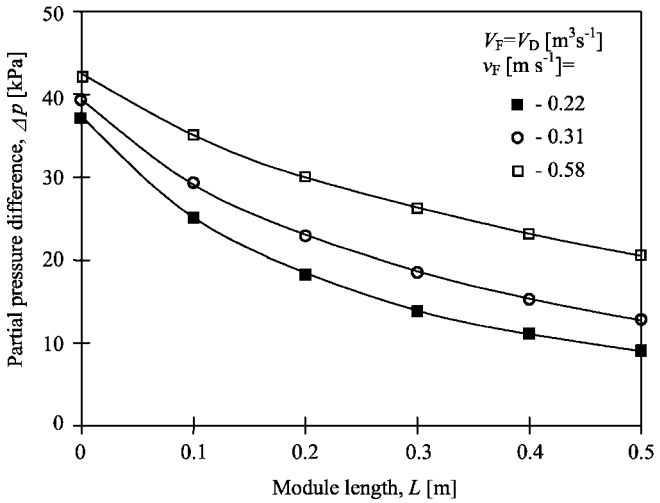

Figure 10. Variation of the mass driving force along the M1 module for different flow velocity. Feed—distilled water. Distillate inlet temperature $T_{Din} = 293$K. Feed inlet temperature $T_{Fin} = 353$K.

The module efficiency is also affected by the concentration polarization. This phenomenon may be reduced by an increase in the flow rate, which improves the mixing conditions inside the module. The average mass transfer coefficient (k_M) calculated for data shown in Fig. 6 increases along with an increase of the flow rate from 5.25×10^{-5} to 15.7×10^{-5} m sec^{-1}, model with the application of Eq. (9). For these values of k_M, the calculated coefficient of concentration polarization (expressed as c_1/c_F) decreased from 1.062 to 1.028. Physicochemical data for NaCl solution necessary for the calculations were taken from Ref. [28].

The feed temperature has a considerable effect on the level of permeate flux in the MD process. At constant distillate temperature (293K) the enhancement of T_F from 348K ($\Delta T_b = T_F - T_D = 55$K) to 358K ($\Delta T_b = 65$K) caused the increase in permeate flux from 400 to 585 dm^3 m^{-2} d^{-1} (Fig. 7—distilled water). Similarly, a 50% increase in permeate flux was obtained for brine. Increasing of distillate temperature causes the reverse effect, that is, declines of permeate flux (Fig. 8). However, the changes of permeate flux are not such pronounced as in the case of feed temperature variation. The dependence of the vapor pressure on temperature is represented by exponential function. Therefore, considerably large changes of Δp as a function of temperature were achieved for feed (high temperature) than those for distillate (low temperature). An analysis of the points

distribution shown in Fig. 8 allows us to conclude, that the efficiency of $400\,dm^3\,m^{-2}\,d^{-1}$ could be achieved for distilled water at the distillate temperature amounting to 323K. This efficiency was estimated for $\Delta T_b = 35K$, which comprises a considerably lower temperature difference than that in the case of feed temperature variations ($\Delta T_b = 55K$, Fig. 7). These results confirmed that the temperature gradient across the membrane is not the real driving force in the MD process. The MD is the diffusion mass transfer process, therefore, the concentration gradient of volatile components in the gas phase ($\Delta y = y_F - y_D$) is a true driving force for the mass transfer. Taking into consideration the relationship between the partial pressure and the mole fraction:

$$y_i = \frac{p_i}{P} \tag{12}$$

where P is the total gas pressure inside the membrane pores, it has been generally accepted to express the driving force in the MD process as the difference of the partial pressures.[7,8,14–17]

Concentration of NaCl Solutions with Crystallization

The solubility of salt increases by only $10\,g\,NaCl\,dm^{-3}$ when the temperature of solution is elevated from 293 to 363K (Fig. 3). Such a small change of the solubility impedes the concentration of NaCl solutions connected with a periodical crystallization (Mode I). Under the operation conditions of the installation in Mode I, it was important to break the MD process run when the salt concentration in the feed reached a value of ca. 320–325 g NaCl dm^{-3}. A rapid increase of hydraulic pressure was observed at the inlet of MD module on the feed side, in the case of higher salt concentration, as a result of salt crystallization inside the capillary membranes. Rinsing the module with distilled water allowed the dissolution of the salt deposit formed. However, the crystallization of salt in the module is disadvantageous since it leads to a rapid wettability of the membrane.[11]

The influence of feed concentration on the efficiency of MD process carried out with periodical crystallization (Mode I) is shown in Fig. 11. An initial salt concentration in the feed was varied in the range 200–237 g NaCl dm^{-3}, and was dependent on the concentration of feeding solution (mother liqueur). During the concentration of these solutions (up to 320–325 g NaCl dm^{-3}) the average permeate flux was maintained at a level of $405\,dm^3\,m^{-2}\,d^{-1}$. Thus, for almost the constant flux of solvent removed from brine, the amount of salt precipitated in the crystallizer increases with an increase of feeding solution concentration.

The literature data[11,26] revealed that the degree of membrane wetting is greater for solutions with higher salt concentration. Therefore, a periodical dilution of solution is advantageous in the MD process carried out according to

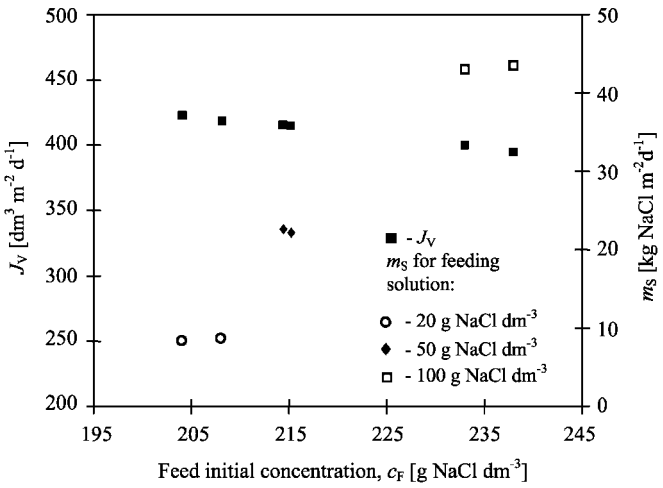

Figure 11. The dependence of the process efficiency (Mode I) as a function of the initial concentration of salt in the feed. Final feed concentration: 320–325 g NaCl dm^{-3}. Feed and distillate inlet temperatures: $T_{Fin} = 358$K and $T_{Din} = 298$K. Flow rates: $v_F = 0.3\,\mathrm{m\,sec^{-1}}$ and $v_D = 0.1\,\mathrm{m\,sec^{-1}}$. Module M1.

Mode I. Changes in M1 module efficiency as a function of the elapsed time are shown in Fig. 12. In the first stage of the studies, distilled water was used as a feed. Measurements were performed in a continuous mode for 5–6 hr/day. Subsequently, the concentration of brine was carried out according to Mode I. A slow decline of the module efficiency was observed during the operation of MD installation. This decline can be attributed to a partial wetting of the membrane by the feed. It was found that the conductivity of the distillate increased from 5 to 30 μS cm^{-1}, as a result of the partial membrane wetting. However, the observed flux decline was not as much significant as it was reported in Ref. [26].

The subsequent investigations of MD were carried out in the system with a continuous crystallization (Mode II). Taking into account the partial wetting of the membranes in M1 module, the experiments were performed with a new M2 module. The experimental results[22] demonstrated that the MD process with continuous crystallization should be carried out at the distillate temperature above 318K. In the case of lower temperatures, a slow increase in the hydraulic pressure at the inlet of MD module on the feed side was observed. It was associated with the crystallization of salt proceeded inside the capillary membranes.

The influence of the feed flow rate in M2 module on the efficiency of MD process integrated with continuous crystallization of salt is shown in Fig. 13. The enhancement of v_F from 0.22 to 0.58 m sec^{-1} caused the increase in both the

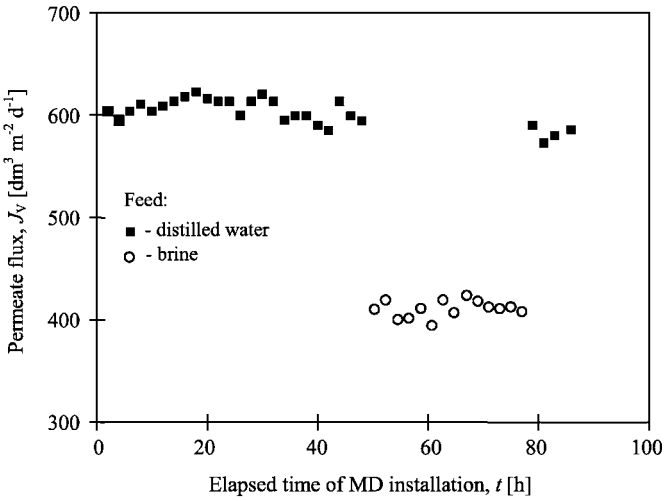

Figure 12. The dependence of the process efficiency on the elapsed time for MD process integrated with periodic salt crystallization (Mode I). Brine—the average concentration 205–240 g NaCl dm^{-3}. Inlet temperatures: $T_{Fin} = 358$K and $T_{Din} = 298$K. Flow rates: $v_F = 0.58$ m sec^{-1} and $v_D = 0.2$ m sec^{-1}. Module M1.

permeate flux (from 150 to 270 dm^3 m^{-2} d^{-1}) and the amount of salt precipitated in crystallizer (from 52 to 91 kg NaCl m^{-2} d^{-1}). These results confirmed a significant influence of the flow rate on the process efficiency. An increase of the flow rate decreased the residence time of feed in each tank of the crystallization system from 10 to 3.5 min, however, this did not pose any operational problem.

The volume losses in the feed stream, for MD process integrated with continuous crystallization, were supplemented by a solution having the concentration from 55 to 315 g NaCl dm^{-3} (Fig. 14). As the salt concentration in the feed increases, together with an increase in feeding solution concentration, a decline of permeate flux was observed. However, the observed flux decline was negligible in comparison to the significant increase in the amounts of salt separated.

Changes of M2 module efficiency during its operation (Fig. 15) indicate that a partial wetting of the membranes also proceeds in this module. The flux was reduced from 270 to 240 dm^3 m^{-2} d^{-1} during 42 hr of module operation. This decline was greater than that observed during the studies with the periodical crystallization (Fig. 12). This confirms the previous results[11] that a high concentration of salt facilitates the membrane wetting. An initial efficiency of the M2 module was recovered by its drying. However, the subsequent measurements with both distilled water and brine demonstrated that rewettability of the membranes took place, similarly to the results from previous work.[11]

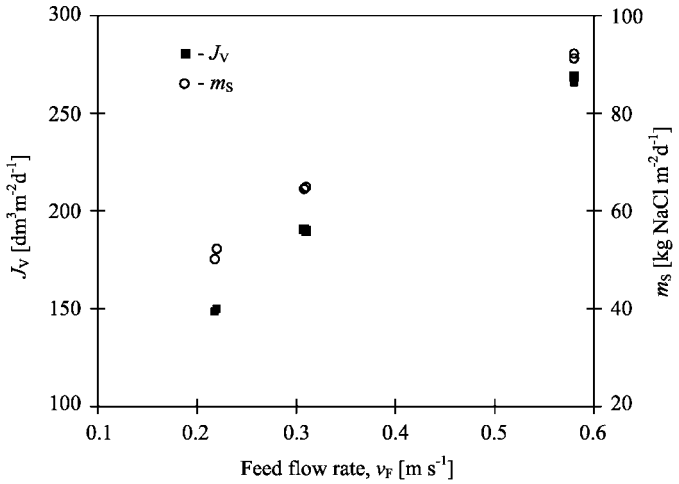

Figure 13. The influence of the feed flow rate on permeate flux and the amount of crystallized salt. The inlet temperatures of streams: $T_{Fin} = 353K$, $T_{Din} = 328K$. Feed—NaCl saturated solution. Module M2.

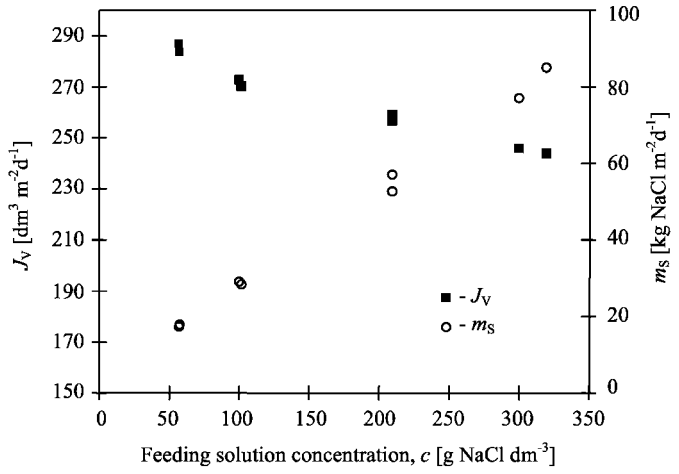

Figure 14. The effects of salt concentration in feeding solution on permeate flux and the amount of crystallized salt in crystallizer (Mode II). The inlet temperatures of streams: $T_{Fin} = 353K$ and $T_{Din} = 328K$. Flow rates: $v_F = 0.58\,m\,sec^{-1}$ and $v_D = 0.2\,m\,sec^{-1}$. Module M2.

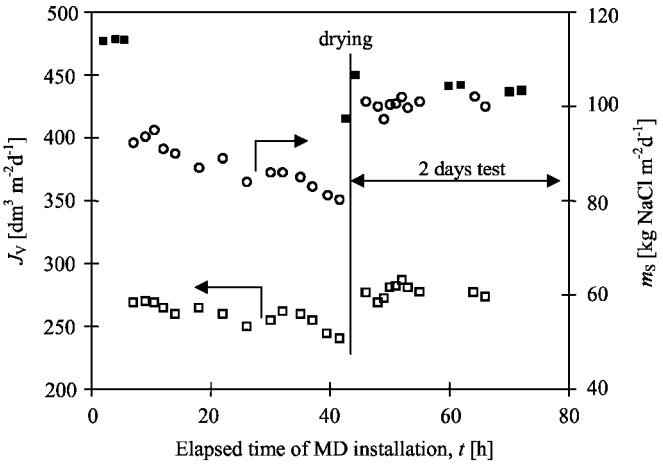

Figure 15. The dependence of the process efficiency on the elapsed time of MD process integrated with salt crystallization (Mode II). J_V, distillate flux for feed; ■, distilled water; □, solution saturated with NaCl; ○, the amount of crystallized salt (m_S). The inlet temperatures of streams: $T_{Fin} = 358$K, $T_{Din} = 328$K. Flow rates: $v_F = 0.3\,\mathrm{m\,sec^{-1}}$ and $v_D = 0.1\,\mathrm{m\,sec^{-1}}$. Module M2.

A slower decline of the efficiency was observed during the studies with M3 module, with a helicoidal flow (Fig. 16). This may be a consequence of two factors. Firstly, the helicoidal flow improves the conditions of mixing in the layer adjacent to the membrane. This results in the reduction of disadvantageous phenomena of the temperature and concentration polarization. Moreover, such conditions make the nucleation of salt more difficult, and consequently the helicoidal flow prevents the formation of salt deposit onto the membrane surface. Secondly, a smaller permeate flux was achieved in M3 module, as a result of lower flow rates of feed and distillate streams. A decrease in the amounts of water evaporated from the membrane surface results in the reduction of the concentration polarization [according to Eq. (6)]. The permeate flux determined for distilled water decreased from 305 to 253 $\mathrm{dm^3\,m^{-2}\,d^{-1}}$ after 110 hr of process duration.

CONCLUSION

The results obtained from the concentration of NaCl solutions by MD revealed that the process is strongly affected by the used parameters. The significant influence on permeate flux was observed for the stream temperatures,

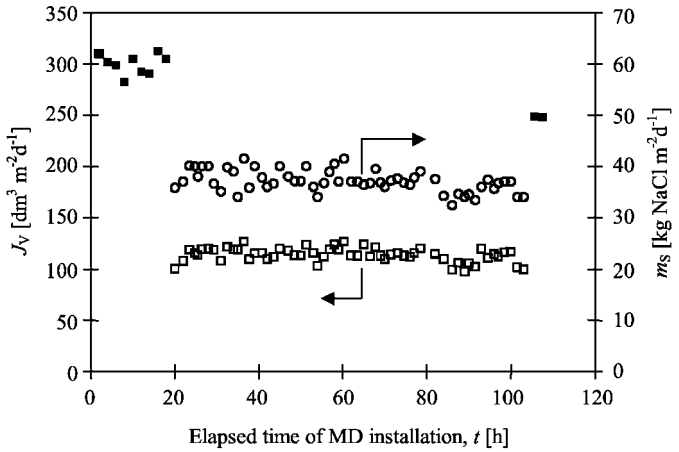

Figure 16. The dependence of the process efficiency on the elapsed time of MD process integrated with salt crystallization (Mode II). J_V, distillate flux for feed; ■, distilled water; □, solution saturated with NaCl; ○, amount of crystallized salt (m_S). The inlet temperatures of streams: $T_{Fin} = 353$K, $T_{Din} = 328$K. Flow rates: $v_F = 0.18\,\mathrm{m\,sec^{-1}}$ and $v_D = 0.03\,\mathrm{m\,sec^{-1}}$. Module M3.

particularly for the feed temperature. Therefore, the application of high-feed temperature, e.g., 358K is advantageous from the point of view of the module efficiency. A decline of permeate flux was found along with enhancement of salt concentration, and for the saturated NaCl solution, the flux was lower by 50% in comparison with that for distilled water. The polarization phenomena have a considerable influence on the MD performance during the concentration of NaCl solutions. Therefore, the flow rate of streams alongside the membrane surface has a great influence on the module efficiency, and the flow rate below $0.5\,\mathrm{m\,sec^{-1}}$ should not be used.

The good agreement between the modeling results and the experimental data was achieved for used MD model. The main source of error in the model analysis was the estimation of the convective heat transfer coefficients. Applying the common Nusselt correlation developed for the tubular heat exchangers, for modeling of used MD modules generates error in the order of 10–30%.

The salt concentration in the feed flowing inside the MD module should not exceed the saturation state for membrane wall temperature. A rapid crystallization of salt on the membrane surface was observed during the concentration of saturated solutions. The maximum bulk concentration of salt in the feed is dependent on both the used process parameters and module design. The solubility of NaCl is slightly dependent on the solution temperature, therefore, the concentration and

temperature polarization may create the saturation state in the vicinity of the membrane surface and facilitate the salt nucleation.

The performed studies (batch mode) revealed that the salt concentration amounting to 320 g dm^{-3} was found to be maximum under used process conditions. The amount of salt separated in the periodic crystallizer was varied in the range 9–43 kg NaCl m^{-2} d^{-1} and was dependent on the feeding solution concentration.

The continuous concentration of saturated solutions can be successfully carried out in a MD installation integrated with the crystallizer. The amount of salt separated in the crystallizer was varied in the range 20–102 kg NaCl m^{-2} d^{-1} and was dependent on the feeding solution concentration as well as on the quantity of water removed from the brine in the MD process.

The membranes were partially wetted during the MD integrated with salt crystallization, which resulted in reduction of permeate flux by 10% after elapsed time of 70 hr (module M2). A solution flowing in the curved tube is subjected to the centrifugal force, and consequently the additional rotary current crosswise to the flow causes a reduction of the polarization phenomena. Thus, the wetting of membranes was significantly reduced in helically wound module (module M3).

NOMENCLATURE

c	concentration (kg m^{-3})
c_p	specific heat (J kg^{-1} K^{-1})
D	diffusion coefficient (m^2 sec^{-1})
d	diameter (m)
d_h	hydraulic diameter (m)
H	vapor enthalpy (J kg^{-1})
J	permeate flux (kg m^{-2} sec^{-1})
J_V	volume permeate flux (m^3 m^{-2} sec^{-1})
k_M	mass transfer coefficient (m sec^{-1})
L	flow channel length (m)
M	molecular weight (kg $kmol^{-1}$)
m_S	amount of crystallized salt (kg NaCl m^{-2} d^{-1})
Nu	Nusselt number
P	total pressure (N m^{-2})
p	partial pressure of saturated vapor over the solution (N m^{-2})
p^0	partial pressure of saturated vapor over the clean solvent (N m^{-2})
Pr	Prandtl number
R	gas constant (J $kmol^{-1}$ K^{-1})
Re	Reynolds number
S	solubility (g dm^{-1})
Sc	Schmidt number

Sh	Sherwood number
s	membrane thickness (m)
T	temperature (K)
V	volume flow rate ($m^3\,sec^{-1}$)
v	flow rate ($m\,sec^{-1}$)
x	mole fraction in liquid phase
y	mole fraction in gas phase

Greek Letters

α	convective heat transfer coefficient ($W\,m^{-2}\,K^{-1}$)
ε	membrane porosity
γ	activity coefficient
ρ	density ($kg\,m^{-3}$)
λ	thermal conductivity coefficient ($W\,m^{-1}\,K^{-1}$)
χ	membrane pore tortuosity
μ	viscosity (Pa sec)

Subscripts

1	boundary layer on the feed side
2	boundary layer on the distillate side
b	bulk
D	distillate
F	feed
in	input
m	membrane
out	output
W	wall

REFERENCES

1. Turek, M.; Mrowiec-Białoń, J.; Gnot, W. Utilization of Coal Mine Brines in the Chlorine Production Process. Desalination **1995**, *101*, 57–67.
2. Turek, M.; Gonet, M. Nanofiltration in the Utilization of Coal-Mine Brines. Desalination **1996**, *108*, 171–177.
3. Masarczyk, J.; Hansson, C.; Solomon, R.; Hallmans, B. Desalination Plant at KWK Debiensko, Poland. Advanced Mine Drainage Water Treatment Engineering for Zero Discharge. Desalination **1989**, *75*, 259–287.
4. Turek, M. Dual-Purpose Desalination-Salt Production System. In *Using Membranes to Assist of Cleaner Processes*, *Proceedings of the XVIII EMS Summer School, Lądek Zdrój, Poland, Sept 9–14, 2001*; Noworyta, A.,

Trusek-Holownia, A., Eds.; Technical University of Wrocław: Poland, 2001; 259–263.
5. Gryta, M. Concentration of Saline Wastewater from the Production of Heparin. Desalination **2000**, *129*, 35–44.
6. Tomaszewska, M. Concentration of the Extraction Fluid from Sulfuric Acid Treatment of Phosphogypsum by Membrane Distillation. J. Membr. Sci. **1993**, *78*, 277–282.
7. Lawson, K.W.; Lloyd, D.R. Membrane Distillation. J. Membr. Sci. **1997**, *124*, 1–25.
8. Tomaszewska, M.; Gryta, M.; Morawski, A.W. The Influence of Salt in Solutions on Hydrochloric Acid Recovery by Membrane Distillation. Sep. Purif. Technol. **1998**, *14*, 183–188.
9. Gryta, M.; Morawski, A.W.; Tomaszewska, M. Ethanol Production in Membrane Distillation Bioreactor. Catal. Today **2000**, *56*, 159–165.
10. Wu, Y.; Kong, Y.; Liu, J.; Zhang, J.; Xu, J. An Experimental Study on Membrane Distillation–Crystallization for Treating Waste Water in Taurine Production. Desalination **1991**, *80*, 235–242.
11. Gryta, M. Direct Contact Membrane Distillation with Crystallization Applied to NaCl Solutions. Chem. Pap. **2002**, *56* (1), 14–19.
12. Gryta, M.; Tomaszewska, M.; Morawski, A.W. Membrane Distillation with Laminar Flow. Sep. Purif. Technol. **1997**, *11*, 93–101.
13. Gryta, M.; Tomaszewska, M.; Morawski, A.W. Erratum. Sep. Technol. **1995**, *5*, 57–59.
14. Gryta, M.; Tomaszewska, M. Heat Transport in the Membrane Distillation Process. J. Membr. Sci. **1998**, *144*, 211–222.
15. Schofield, R.W.; Field, A.G.; Fell, C.J.D.; Macoun, R. Factor Affecting Flux in Membrane Distillation. Desalination **1990**, *77*, 279–294.
16. Tomaszewska, M.; Gryta, M.; Morawski, A.W. Study on the Concentration of Acids by Membrane Distillation. J. Membr. Sci. **1995**, *102*, 113–122.
17. Garcia-Payo, M.C.; Izquierdo-Gil, M.A.; Fernández-Pineda, C. Air Gap Membrane Distillation of Aqueous Alcohol Solutions. J. Membr. Sci. **2000**, *169*, 61–80.
18. Holman, J.P. *Heat Transfer*, 8th Ed.; McGraw-Hill: New York, 1997.
19. Izquierdo-Gil, M.A.; Garcia-Payo, M.C.; Fernández-Pineda, C. Direct Contact Membrane Distillation of Sugar Aqueous Solutions. Sep. Sci. Technol. **1999**, *34*, 1773–1801.
20. Hobler, T. *Heat Transfer and Heat Exchangers*; WNT: Warsaw, 1986 (in Polish).
21. Gryta, M.; Tomaszewska, M. The Capillary MD Module Integrated with a Heat Exchanger. Inz. Chem. Proc. **1999**, *20*, 221–233.
22. Gryta, M.; Tomaszewska, M.; Morawski, A.W. A Capillary Module for Membrane Distillation Process. Chem. Pap. **2000**, *54* (6a), 370–374.

23. Ophoff, J.; Vos, G.S.; Rácz, I.G.; Reith, T. Flux Enhancement by Reduction of Concentration Polarisation Due to Secondary Flow in Twisted Membrane Tubes. In *Progress in Membrane Science and Technology*, *Proceedings of the III International Symposium Euromembrane '97, University of Twente, June 23–27 1997*; Kempermen, A.J.B., Koops, G.H., Eds.; Enschede: The Netherlands, 1997; 400–403.
24. Gabelman, A.; Hwang, S.T. Hollow Fiber Membrane Contactors. J. Membr. Sci. **1999**, *159*, 61–106.
25. Banat, F.A.; Simandl, J. Theoretical and Experimental Study in Membrane Distillation. Desalination **1994**, *95*, 39–52.
26. Cheng, D.Y.; Wiersma, S.J. Composite Membrane for Membrane Distillation System, US Patent 4,419,242, December 6, 1983.
27. Lide, D.R. (Ed.) *CRC Handbook of Chemistry and Physics*, 78th Ed.; CRC Press: New York, 1997.
28. Morton, R.; Smith, J., (Eds.) *Saline Water Conversion Engineering Data Book*, 2nd Ed.; The M.W. Kellogg Company: Washington, 1971.

Received January 2002
Revised April 2002